

**Scaling during shadowing growth of isolated nanocolumns**

T. Karabacak, J. P. Singh, Y.-P. Zhao, G.-C. Wang, and T.-M. Lu

*Department of Physics, Applied Physics and Astronomy, Rensselaer Polytechnic Institute, Troy, New York 12180-3590, USA*

(Received 29 April 2003; revised manuscript received 15 July 2003; published 12 September 2003)

We observed a scaling behavior during the shadowing growth of isolated Si, Co, Cu, and W nanocolumnar structures on Si substrates using the oblique angle deposition with substrate rotation (also known as glancing angle deposition or simply GLAD). The width of the isolated columns,  $W$ , grew as a function of column length,  $d$ , in a power law form,  $W \sim d^p$ , where  $p$  is the growth exponent and was measured to be  $\sim 0.28$ – $0.34$ . It is argued that shadowing without diffusion should lead to  $p = 0.50$  and would cross over to  $0.31$  if one considers surface diffusion. It is of great interest to determine the mechanisms that would affect the value of  $p$  since it is an important factor that would control the shape, final size, and spacing of the isolated nanocolumns eventually produced.

DOI: 10.1103/PhysRevB.68.125408

PACS number(s): 68.55.Jk, 68.35.Ct, 81.07.-b, 81.15.Aa

**INTRODUCTION**

There has been intense interest in the study of the dynamics of surface and interface morphology evolution in recent years. On the one hand, the surface and interface phenomena often occur at far-from-equilibrium, an area of fundamental interest to scientists.<sup>1</sup> On the practical side, it has been shown recently that many intriguing properties can be created out of unusually rough surfaces and interface structures<sup>2,3</sup> that have many positive impacts, and may lead to many new applications in mechanical, optical, electrical, and biological devices, as well as in the medical field.

A particularly interesting way to generate such structures is by physical shadowing during an oblique angle deposition.<sup>1</sup> In this technique, incoming atoms arrive at the substrate surface at a large angle  $\theta$  with respect to the surface normal. Due to the shadowing effect, the incident flux of a material is preferentially deposited on the top of surface features with larger surface heights during the initial nucleation. This effect would eventually lead to the creation of isolated nanocolumns. In the case where the substrate remains stationary during growth, it has been shown that shadowing would lead to interesting scaling behavior of the isolated nanocolumnar structures.<sup>4</sup> More recently, oblique angle deposition with substrate rotation (also known as the glancing angle deposition) has attracted great attention<sup>2,3</sup> due to its ability to generate many diverse surface nanostructures. Thus far, some simulation work has been reported to describe qualitatively the formation of the three-dimensional structures.<sup>5,6</sup> Very little work has been performed to predict the growth behavior of these structures quantitatively.

In this paper we report quantitative measurements on the evolution of the silicon, copper, cobalt, and tungsten isolated nanocolumnar structures induced by the shadowing effect during the oblique angle deposition with substrate rotation. We found that initially the width  $W$  of the isolated columns grew as a function of time, or equivalently, as a function of column length  $d$ , in a power law form,  $W \sim d^p$ , where  $p \sim 0.28$ – $0.34$ . The result is consistent with our simulations by including both shadowing and surface diffusion effects. We also argue that shadowing without diffusion would lead to

$p = 0.50$ , and will cross over to  $0.31$  if one considers a sufficiently large surface diffusion.

**EXPERIMENT**

We used a thermal evaporation system to deposit Si, Cu, and Co columnar films. W films were deposited by a sputter deposition unit. All the substrates were polished  $p$ -Si(100) (resistivity 12–25  $\Omega$  cm). The substrates were RCA cleaned,<sup>7</sup> and an oxide layer was formed on the substrate surface. All the films were then deposited on these surfaces using the oblique angle deposition technique. During our oblique angle depositions, the substrate was tilted so that the angle between the surface normal of the target and the surface normal of the substrate could be large. The rotation of the substrates was driven by a computerized step motor and the rotation speed was set to 0.5 Hz (30 rpm).

The deposition by thermal evaporation was performed in a vacuum chamber with a base pressure of  $\sim 2 \times 10^{-6}$  Torr with a diffusion pump. The deposition angle which was defined to be the angle between the incident flux and the substrate surface normal was set to  $\theta = 85^\circ$ . The target-to-substrate distance was  $\sim 32$  cm. The target material inside a crucible is thermally evaporated by the bombardment of highly energetic electrons. The deposition rate was controlled using a crystal quartz monitor, and set to be  $\sim 0.5$  nm/s. The deposition was performed at near room temperature (no intentional heating of the substrate).

We used a dc magnetron sputtering system to deposit our columnar tungsten films. The target was a 99.95% pure W cathode (diameter  $\sim 7.6$  cm). The substrates were mounted on a sample holder located at a distance of 15 cm from the cathode with a deposition angle of  $\theta = 87^\circ$ . The base pressure of  $\sim 2 \times 10^{-6}$  Torr was achieved by a turbomolecular pump backed by a mechanical pump. During the sputter deposition, the power was 200 W at an Ar (ultrahigh purity) pressure of 1.5 mTorr. The deposition rate was measured to be  $\sim 0.08$  nm/sec by step profilometry and verified by scanning electron microscopy (SEM) cross-sectional images. The maximum temperature of the substrate during the sputter deposition was found to be  $\sim 85^\circ$  C.

The deposited films were imaged using a field emission SEM (SEM-6330F, Jeol Ltd., Tokyo, Japan). A tungsten tip

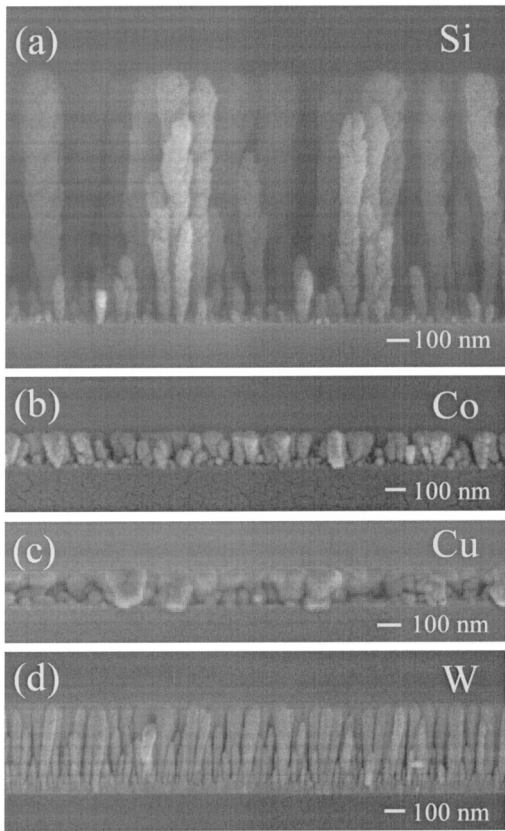


FIG. 1. Cross-sectional scanning electron micrographs of isolated nanocolumnar structures: (a) Si, (b) Co, (c) Cu, and (d) W. The scale bar is 100 nm.

was heated and a 5-kV accelerating voltage was applied to release electrons in the SEM measurements. The emission current ranged from 10.5 to 12.5  $\mu\text{A}$  during operating, and the working distance was about 10 mm.

After an initial random nucleation of islands on the surface, the incident flux is preferentially deposited on top of these islands and no atom can reach the valleys between islands due to the shadowing effect. Isolated columns therefore are formed on these islands during subsequent growth.

In Fig. 1 we show the cross section of scanning electron micrographs of representative Si, Co, Cu, and W films. As we can see in Fig. 1, after an initial nucleation of islands, the dominant columns grow as a function of time while some secondary columns stop growing. A salient feature of these columnar structures is that the width  $W$  of these columns appears to grow in time, or the length of the column,  $d$ . To study quantitatively the growth behavior of the columns, in Fig. 2 we plot (on a log-log scale), the width  $W$  as a function of  $d$ . The length scale of the SEM image was first calibrated, and then the width  $W$  and length  $d$  of the columns were measured. Each data point is the average of measurements on 6–10 columns. Each error bar on the measured column width on the curve represents the standard deviation of measured values. A linear relationship for all the columns of different materials is found in this plot. The growth is interpreted as a power law growth with the relationship  $W \sim d^p$ , where  $p \sim 0.28\text{--}0.34$  is the growth exponent.

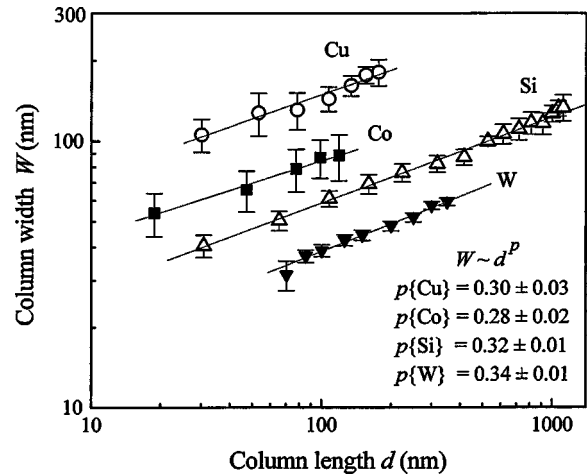


FIG. 2. The average column width  $W$  data are plotted as a function of column length  $d$  for the materials (Cu, Co, Si, and W) studied. Each data point is the average of measurements on 6–10 columns. Each error bar on the measured column width on the curve represents the standard deviation of the measured value.

SIMULATIONS

In order to understand this growth behavior we use a three-dimensional Monte Carlo method to simulate the growth of the columns produced by the oblique angle deposition. As illustrated in Fig. 3, a three-dimensional lattice, which allows overhangs, is formed by cubic lattice points, and each incident atom has the dimension of one lattice point. The simulations include an obliquely incident flux, a substrate rotation, and surface diffusion. Surface diffusion has been shown to be a critical factor during the formation of columnar structures of oblique angle deposition.<sup>8,9</sup> We assume a uniform flux of atoms approaching the surface with an angle  $\theta = 85^\circ$ . At each simulation step an atom is sent towards a randomly chosen lattice point on the surface of size  $L \times L$ . To take into account the substrate rotation, each atom is sent with a change in the azimuthal angle of  $\Delta\phi = 0.036^\circ$  from the previous one. After the incident atom is deposited onto the surface, an atom that is chosen randomly within a box around the impact point is set to diffuse to another nearest neighbor random location. The diffusion step is repeated until  $D$  number of jumps is made. Then another atom is sent, and the deposition and diffusion steps are repeated in the similar way. This strategy mimics the surface

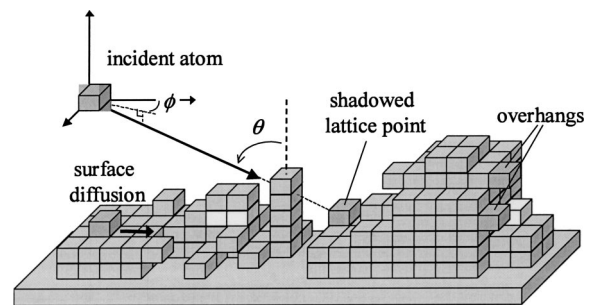


FIG. 3. A schematic of three-dimensional Monte Carlo simulations for oblique angle deposition.

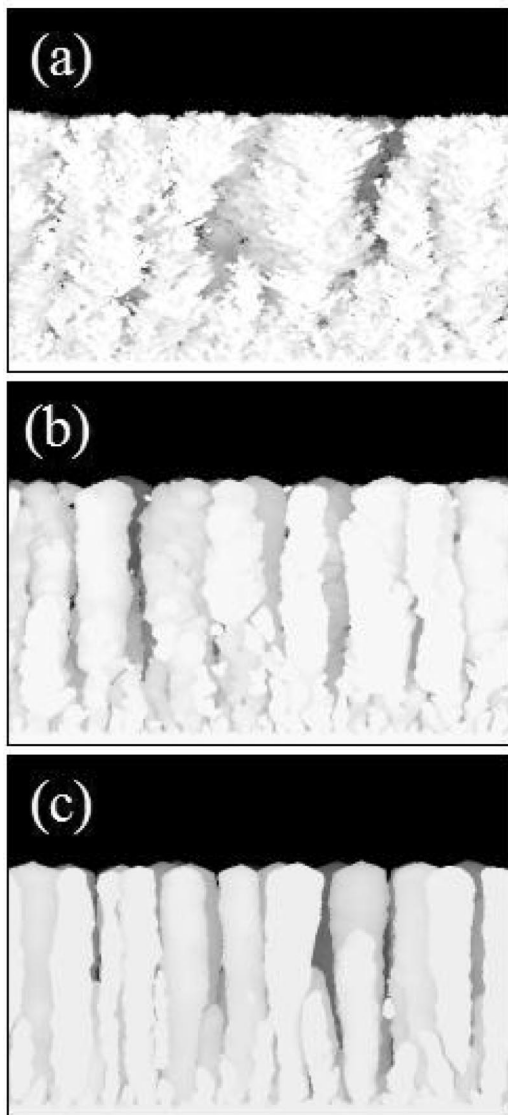


FIG. 4. Cross-sectional images of simulated columns by a three-dimensional Monte Carlo code are presented for various surface diffusion rates  $D$ : (a)  $D=20$ , (b)  $D=100$ , and (c)  $D=500$ . The lateral full scale is 512 lattice units in our Monte Carlo simulations.

diffusion at the first impact point during the growth by evaporation deposition. It is similar to previous simulation work on surface diffusion during growth.<sup>10,11</sup>

Our simulations typically involved a system size of  $L \times L \times N = 512 \times 512 \times 512$ , with a periodic boundary condition. The simulations were conducted for different values of  $D$  ranging from 0 to  $4 \times 10^3$ . After each simulation,  $W$  as a function of  $d$  is calculated by slicing the film layer by layer parallel to the substrate plane. Figure 4 shows representative simulated cross sections with increasing rates from (a) to (c). It is realized that when the diffusion rate approaches zero, columns are fractal-like and it is difficult to define column borders. On the other hand, as we increase the diffusion rate, we start to get columns with smoother borders and they look very much like the experimentally obtained nanocolumns. Diffusion is shown to improve the columnar structure by making columns denser and column edges smoother. Figure

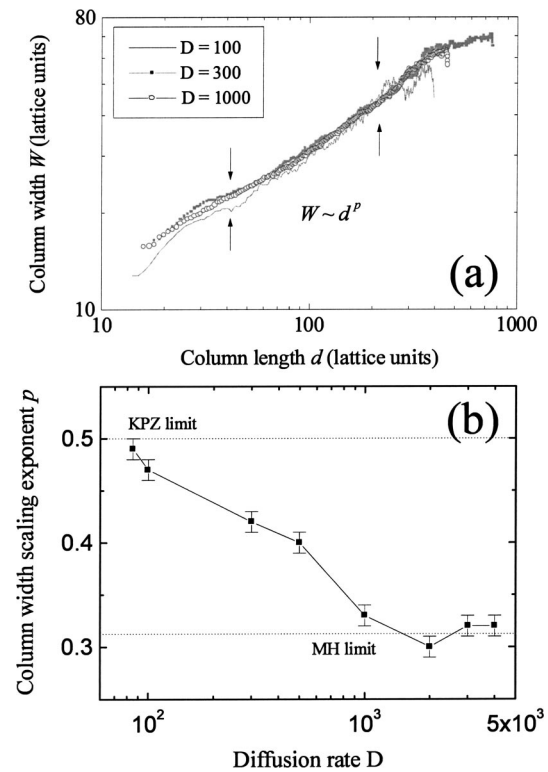


FIG. 5. (a) Simulated column average widths as a function of column length are plotted for the columns at various diffusion rates,  $D=100$ , 300, and 1000. The vertical arrows indicate the regime used for determining the scaling exponent. (b) Scaling exponent  $p$  calculated for eight surface diffusion rates are shown. The dotted lines represent the KPZ and MH limits obtained by analytic solutions.

5(a) plots the change of  $W$  as a function of  $d$  for various diffusion rates. The log-log plot reveals that the simulated column widths also have a power law dependence on  $d$ . The exponent  $p$  at a given  $D$  is shown in Fig. 5(b). When the diffusion rate approaches zero,  $p$  is found to approach 0.5. With increasing diffusion rates, the value of  $p$  “crosses over” from 0.5 to 0.3. Our experimental values of  $p$  are in between 0.5 and 0.3, but closer to 0.3. We therefore believe that our simulation results are consistent with our experimental measurements.

#### ANALYTICAL MODEL

Meakin and Krug reported earlier their theoretical study on the oblique angle deposition ( $\theta$  approaches  $90^\circ$ ) without substrate rotation.<sup>4</sup> Surface diffusion was not included in their study. They investigated the evolution of column edges when the columns were cross sectioned through a plane parallel to a substrate. They found that “cluster edges evolve according to a growth process reminiscent of the two-dimensional Eden model, and hence their fluctuations can be described by the well-known Kardar-Parisi-Zhang (KPZ) equation for a one-dimensional moving interface.” As also illustrated in Fig. 6, they identified the surface correlation lengths  $\xi_x$  and  $\xi_y$  to be the column widths in the  $x$  and  $y$  directions parallel to the substrate, respectively. The incident

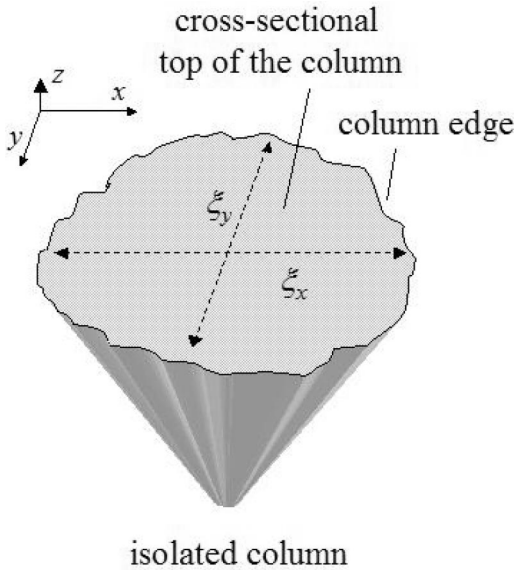


FIG. 6. A schematic of an isolated column with a cross-sectioned top view.  $\xi_x$  and  $\xi_y$  are column widths along the  $x$  and  $y$  directions, respectively.

beam on the substrate is in the  $x$  direction and is perpendicular to the  $y$  direction. These column widths were shown to correspond to the correlation lengths of the  $(1+1)$ -dimensional KPZ interface,<sup>12</sup> with  $\xi_x \sim d^{p_x}$ , and  $\xi_y \sim d^{p_y}$ , where

$$p_x(\text{KPZ}) = \frac{1}{3} \quad \text{and} \quad p_y(\text{KPZ}) = \frac{2}{3}.$$

These results are applicable when the substrate stays stationary during a deposition. In our case of substrate rotation one would expect  $W \sim \sqrt{\xi_x \xi_y} \sim \sqrt{d^{p_x + p_y}} = d^{(p_x + p_y)/2} \equiv d^p$ , with the scaling exponent

$$p(\text{KPZ}) = \frac{(p_x + p_y)}{2} = \frac{1/3 + 2/3}{2} = \frac{1}{2} = 0.50.$$

(The cross section area of the column is the product of  $\xi_x$  and  $\xi_y$ .) Therefore, only one growth exponent is required to describe the growth and the structure is symmetric in the  $x$  and  $y$  directions.

By using a similar argument we can incorporate the effect of diffusion by starting with the  $(1+1)$ -dimensional model of Mullins-Herring (MH).<sup>13</sup> In the MH model, surface diffusion and noise are the mechanisms that control the growth and would give

$$p_x(\text{MH}) = \frac{3}{8} \quad \text{and} \quad p_y(\text{MH}) = \frac{1}{4},$$

when the substrate stays stationary during a deposition. For the present case of substrate rotation, we thus have

$$p(\text{MH}) = \frac{(p_x + p_y)}{2} = \frac{3/8 + 1/4}{2} = \frac{5}{16} \sim 0.31.$$

Therefore in the  $(2+1)$ -dimensional oblique angle deposition with substrate rotation, we expect the column width scaling exponent should cross over from  $p(\text{KPZ}) = 0.50$  for pure shadowing with no diffusion to  $p(\text{MH}) = 0.31$  for both shadowing and surface diffusion. Also, our simulation results agree well with these estimations [see Fig. 5(b), dotted lines]. There exists a competition between shadowing and diffusion. Shadowing tends to make columns grow wider while diffusion forces columns to grow towards the columnar axes.

## CONCLUSIONS

In conclusion, we have shown that there is a scaling relationship for the evolution of the isolated columnar width of various materials with column length during an oblique angle deposition with substrate rotation. We showed that the column width changes with the column length according to a power law with the exponent  $p \sim 0.28-0.34$ . It is argued that the growth exponent should cross over from 0.50 with pure shadowing, and that there is no surface diffusion to 0.31 with both shadowing and surface diffusion. Since the value of  $p$  is an important factor that controls the shape, size, and spacing of the final columns, it is of great interest to understand the mechanisms that determine the exponent value.

## ACKNOWLEDGMENTS

This work was supported in part by the NSF. T.K. was supported by the Harry F. Meiners Fellowship. We thank G.-R. Yang, Y.-G. Zhao, and A. Vijayaraghavan for assisting with the deposition and D.-X. Ye for taking the scanning electron micrographs of the samples.

<sup>1</sup>P. Meakin, *Fractals, Scaling, and Growth Far from Equilibrium* (Cambridge University Press, Cambridge, 1998), pp. 408–411 and 553–569.

<sup>2</sup>K. Robbie, M.J. Brett, and A. Lakhtakia, *Nature (London)* **384**, 616 (1996).

<sup>3</sup>Y.-P. Zhao, D.-X. Ye, G.-C. Wang, and T.-M. Lu, *Nano Lett.* **2**, 351 (2001).

<sup>4</sup>P. Meakin and J. Krug, *Europhys. Lett.* **11**, 7 (1990); P. Meakin

and J. Krug, *Phys. Rev. A* **46**, 3390 (1992).

<sup>5</sup>R. Messier, V.C. Venugopal, and P.D. Sunal, *J. Vac. Sci. Technol. A* **18**, 1538 (2000).

<sup>6</sup>T. Smy, D. Wakley, K.D. Harris, and M.J. Brett, *Thin Solid Films* **391**, 88 (2001).

<sup>7</sup>S.A. Campbell, *The Science and Engineering of Microelectronic Fabrication* (Oxford University Press, New York, 1996), p. 341.

<sup>8</sup>S. Lichter and J. Chen, *Phys. Rev. Lett.* **56**, 1396 (1986).

- <sup>9</sup>S.G. Mayr and K. Samwer, *J. Appl. Phys.* **91**, 2779 (2002).
- <sup>10</sup>J.G. Amar, F. Family, and P.-M. Lam, *Phys. Rev. B* **50**, 8781 (1994).
- <sup>11</sup>T. Karabacak, Y.-P. Zhao, G.-C. Wang, and T.-M. Lu, *Phys. Rev. B* **64**, 085323 (2001); **66**, 075329 (2002).
- <sup>12</sup>M. Kardar, G. Parisi, and Y.-C. Zhang, *Phys. Rev. Lett.* **56**, 889 (1986).
- <sup>13</sup>A.-L. Barabasi and H. E. Stanley, *Fractal Concepts in Surface Growth* (Cambridge University Press, Cambridge, 1995), p. 142.